



RESEARCH ARTICLE

# Urine-based Detection of Congenital Portosystemic Shunt in C57BL/6 Mice

Beng San Yeoh<sup>1</sup>, Rachel M. Golonka<sup>1</sup>, Piu Saha<sup>1</sup>, Mrunmayee R. Kandalgaonkar<sup>1</sup>, Yuan Tian<sup>2</sup>, Islam Osman<sup>1</sup>, Andrew D. Patterson <sup>2</sup>, Andrew T. Gewirtz<sup>3</sup>, Bina Joe<sup>1,\*</sup>, Matam Vijay-Kumar <sup>1,\*</sup>

<sup>1</sup>Department of Physiology and Pharmacology, The University of Toledo College of Medicine and Life Sciences, Toledo, OH 43614, USA, <sup>2</sup>Department of Veterinary and Biomedical Sciences, The Pennsylvania State University, University Park, PA 16802, USA and <sup>3</sup>Center for Inflammation, Immunity & Infection, Institute for Biomedical Sciences, Georgia State University, Atlanta, GA 30303, USA

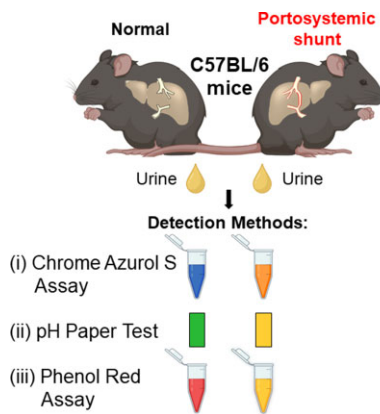
\*Address correspondence to M.V.-K. (e-mail: [matamvijaykumar@utoledo.edu](mailto:matamvijaykumar@utoledo.edu)), B.J. (e-mail: [bina.joe@utoledo.edu](mailto:bina.joe@utoledo.edu))

## Abstract

Sporadic occurrence of congenital portosystemic shunt (PSS) at a rate of ~1 out of 10 among C57BL/6 J mice, which are widely used in biomedical research, results in aberrancies in serologic, metabolic, and physiologic parameters. Therefore, mice with PSS should be identified as outliers in research. Accordingly, we sought methods to, reliably and efficiently, identify PSS mice. Serum total bile acids  $\geq 40 \mu\text{M}$  is a *bona fide* biomarker of PSS in mice but utility of this biomarker is limited by its cost and invasiveness, particularly if large numbers of mice are to be screened. This led us to investigate if assay of urine might serve as a simple, inexpensive, noninvasive means of PSS diagnosis. Metabolome profiling uncovered that Krebs cycle intermediates, that is, citrate,  $\alpha$ -ketoglutarate, and fumarate, were strikingly and distinctly elevated in the urine of PSS mice. We leveraged the iron-chelating and pH-lowering properties of such metabolites as the basis for 3 urine-based PSS screening tests: urinary iron-chelation assay, pH strip test, and phenol red assay. Our findings demonstrate the feasibility of using these colorimetric assays, whereby their readout can be assessed by direct observation, to diagnose PSS in an inexpensive, rapid, and noninvasive manner. Application of our urinary PSS screening protocols can aid biomedical research by enabling stratification of PSS mice, which, at present, likely confound numerous ongoing studies.

Submitted: 7 July 2023; Revised: 22 July 2023; Accepted: 25 July 2023

© The Author(s) 2023. Published by Oxford University Press on behalf of American Physiological Society. This is an Open Access article distributed under the terms of the Creative Commons Attribution-NonCommercial License (<https://creativecommons.org/licenses/by-nc/4.0/>), which permits non-commercial re-use, distribution, and reproduction in any medium, provided the original work is properly cited. For commercial re-use, please contact [journals.permissions@oup.com](mailto:journals.permissions@oup.com)



**Key words:** liver shunt; bile acids; enterohepatic circulation; Krebs cycle; pH; iron chelation

## Introduction

The biomedical community has vastly invested in generating numerous genetically engineered knockout, knock-in, and transgenic mice on the C57BL/6 J background, an inbred mouse strain that is widely used in basic scientific research. Despite such use of an inbred strain greatly reduces genetic heterogeneity, some C57BL/6 J mice still exhibit stark phenotypic aberrations, including the sporadic prenatal development of portosystemic shunt (PSS; an abnormal vein that connects portal vascular system with systemic circulation).<sup>1</sup> This is alarming considering that the prevalence of PSS among C57BL/6 J [alias wild-type (WT)] mice is ~8%–15%<sup>2</sup> and could be higher ( $\geq 40\%$ ) in certain genetically modified C57BL/6 J mice.<sup>3–7</sup> On one hand, PSS may present a significant confounding variable that should be excluded, or at least stratified from many studies to yield more precise and reliable conclusion. Of note, PSS mice may pose as confounders due to their abnormal neurochemical profile,<sup>1</sup> altered drug and toxicological response,<sup>5,8</sup> metabolic perturbations (eg, hypocholesterolemia, hypotriglyceridemia, and hypoglycemia),<sup>2,9</sup> and an intolerance to purified diets that trigger rapid onset of cholestatic liver injury<sup>10</sup> and cancer.<sup>2,3</sup> On the other hand, murine PSS can be harnessed as the sought-after animal model for understanding the mechanisms and pathophysiology of human PSS. Screening for PSS in mice, however, remains challenging due to its asymptomatic nature and the lack of diagnostic tests that allow its identification in a high-throughput manner.<sup>2,10</sup>

Contemporary methods for diagnosing PSS in mice currently rely on either time-lapsed portal angiography or portal vein perfusion with dye, resin, or fluorescent microspheres.<sup>1,4,5,11</sup> These diagnostic tests are invasive, terminal procedures and therefore are ill-suited for use in identifying viable mice for further studies. Previously, we have optimized a nonterminal screening procedure, that is, quantification of serum total bile acids (TBA) as a *bona fide* marker of PSS, to discern mice with or without this vascular anomaly as early as 15 d of age.<sup>2</sup> Notwithstanding that high serum TBA is 100% accurate in diagnosing PSS, it has 2 limitations: (i) blood collection is invasive and stressful for the mice, and requires expertise in acquiring hemolysis-free sera, and (ii) serum TBA assay requires a spectrophotometer and thus could not be performed on-site in the vivaria. Accordingly, there is an unmet need to determine methodologies that allow for simple, rapid, and cost-effective identification of mice with PSS. Herein, we leveraged the use of urine as a readily accessible liquid biopsy

and evaluated colorimetric tests for identifying mice with or without PSS.

## Materials and Methods

### Mice

C57BL/6 J WT mice (Stock# 000664), mice expressing the *Ahr* floxed allele (*Ahr*<sup>fl/fl</sup>; Stock# 006203), and mice expressing a Cre recombinase driven by vascular endothelial cadherin (*Cdh5*) promoter (*Cre*<sup>Cdh5</sup>; Stock# 006137) were procured from the Jackson Laboratory and bred in-house in the Department of Laboratory Animal Resources, University of Toledo College of Medicine and Life Sciences. *Ahr*<sup>fl/fl</sup> mice were crossed with *Cre*<sup>Cdh5</sup> mice to generate endothelial-specific AHR deficient mice (*Ahr*<sup>fl/fl</sup>*Cre*<sup>Cdh5</sup>). *Ahr*<sup>fl/fl</sup> littermates were used as controls for *Ahr*<sup>fl/fl</sup>*Cre*<sup>Cdh5</sup> mice. Swiss Webster mice (model# SW) were obtained from the Taconic Biosciences and bred in-house. Mice were maintained under specific-pathogen-free conditions, housed in cages containing corn-cob bedding (Bed-O-Cob, The Andersons Co.) and nestlets (Cat# CABFM00088, Ancare Corp.) and fed ad libitum grain-based chow (LabDiet 5001). Mice were housed at 23°C with 12 h light/dark cycle. The Institutional Animal Care and Use Committee (IACUC) at The University of Toledo approved all mouse experiments.

### PSS Screening Using Serum TBA Quantification

We have previously described serum TBA as a biomarker of PSS, where levels  $\geq 40 \mu\text{M}$  upon 2 repeated sampling were indicative of PSS in mice.<sup>2</sup> Briefly, blood from day 15 old male and female mice ( $n = 50\text{--}60$ ) was collected minimally via mandibular bleeding into serum-separating tubes (BD Biosciences). After centrifugation, hemolysis-free sera were collected and measured for serum TBA using a TBA assay kit (Enzyme Cycling Method; Diazyme Laboratories) according to manufacturer's protocol. Mice identified as non-PSS or PSS ( $n = 6$ ) in this manner were bled and measured for serum TBA again at 8-wk-old.

### Urine Collection

Mice (8-wk-old male and female) fed ad libitum were placed on a clean aluminum foil and then restrained by gripping the loose skin around the neck. This prompts mice to urinate, whereby their urine was collected directly into microcentrifuge tubes or

pipetted from the aluminum foil. Urine samples were stored in  $-80^{\circ}\text{C}$  until further analyses.

### Urinary TBA Quantification

Urinary TBA was measured using a TBA assay kit (Enzyme Cycling Method; Diazyme Laboratories) according to the manufacturer's protocol.

### Vascular Casting of PSS

Resin casting of liver vasculature was employed for postmortem confirmation of PSS. Briefly, 400  $\mu\text{L}$  of Mercor II resin mixed with 5% benzoyl peroxide (Ladd Research) was injected into the portal vein with a 30-gauge, 0.5-inch needle. Resin was allowed to solidify at room temperature for 30 min and then the liver was resected and immersed in 15% potassium hydroxide overnight. Vascular cast was carefully rinsed with water and imaged for the presence of PSS.

### Urine Nuclear Magnetic Resonance Spectroscopy (NMR) Analysis

Urine samples collected from 24-wk-old C57BL/6 J male mice were processed as described previously for NMR analysis.<sup>12</sup> Briefly, urine sample (100  $\mu\text{L}$ ) was mixed with 400  $\mu\text{L}$  of 50%  $\text{D}_2\text{O}$  and 50  $\mu\text{L}$  of phosphate buffer (1.5 M,  $\text{K}_2\text{HPO}_4\text{:NaH}_2\text{PO}_4 \approx 4:1$ ,  $\text{pD} \approx 7.4$ ), containing 100%  $\text{D}_2\text{O}$  as a field lock signal and 0.05% TSP (sodium 3-trimethylsilyl-2,2,3,3-tetradeuteropropionate) as a chemical shift reference. After centrifugation at 16,090  $g$  ( $4^{\circ}\text{C}$ , 10 min), 500  $\mu\text{L}$  of supernatant was transferred into a 5 mm NMR tube for NMR spectral acquisition.  $^1\text{H}$ -NMR spectra were recorded at 298 K using a Bruker AVANCE NEO 600 MHz NMR spectrometer (Bruker Biospin, German). Multivariable data analysis was carried out with the SIMCAP + software (version 13.0, Umetrics, Sweden) and MATLAB (The Mathworks Inc., Natwick, MA).

### Chrome Azurol S (CAS) Assay

CAS assay was used to assess the activity of iron chelators (*alias* siderophores) present in biological samples, which turn CAS from blue to orange in color. Reagents for both CAS agar plate and liquid assays were prepared as described by Schwyn and Neilands.<sup>13</sup> For the agar plate assay, 3  $\mu\text{L}$  of urine and known concentrations of sodium citrate (1, 10, 50, and 100 mM) (Alfa Aesar) were spotted on the agar plate and incubated for 1 h at room temperature. The intensity of orange halo formation was proportional to the degree of iron chelation from CAS agar plate. For the liquid assay, urine was diluted in water (1:100) and 100  $\mu\text{L}$  was added to a 96-well plate. CAS reagent (100  $\mu\text{L}$ ) was added to the wells, incubated for 40 min at room temperature, and the absorbance was read at the wavelength of 630 nm using a spectrophotometer. Results were expressed as % change in absorbance readings of samples relative to vehicle control (water). In a separate experiment, to confirm that the colorimetric change is specifically due to iron chelation, urine samples were spiked with increasing concentrations of  $\text{FeCl}_3 \cdot 6\text{H}_2\text{O}$  to neutralize iron chelation. Briefly, 50  $\mu\text{L}$  of  $\text{FeCl}_3$  solution (prepared at 0, 0.4, 1, 2, or 4 mM working stock concentration) were added to 50  $\mu\text{L}$  of urine diluted in water (1:50) in a 96-well plate. Vehicle controls for each of the iron concentrations were prepared by replacing urine with water. CAS reagent (100  $\mu\text{L}$ ) was added to the wells, incubated for 40 min at room temperature,

and the absorbance was read at the wavelength of 630 nm using a spectrophotometer. Results were expressed as % change in absorbance readings of samples relative to vehicle control group spiked with their corresponding concentration of  $\text{FeCl}_3$ .

### Urinary pH Estimation Using pH Test Strips

Urinary pH was measured using Hydriion pH test strips with a narrow range of pH 5.5–8.0 (Cat# 067; Micro Essential Laboratory, NY).

### Urinary pH Estimation Using Phenol Red

Phenol red solution (0.1 mg/mL) was prepared in water and adjusted to pH 7.4 using 1 M sodium hydroxide. Urine samples (2.0  $\mu\text{L}$ ) were added to a 96-well plate, followed by 200  $\mu\text{L}$  of phenol red solution. The wells were gently tapped to ensure thorough mixing and the absorbance was read at the wavelength of 560 nm using a spectrophotometer. To determine detection limit, urine was serially diluted (2-fold) in phenol red solution until the assay could no longer detect differences between PSS from non-PSS samples. Assay accuracy, sensitivity, and specificity were calculated in comparison to postmortem confirmation of PSS via vascular casting, as well as in comparison to serum TBA. As described previously,<sup>14</sup> accuracy is defined as proportion of true positive and true negative in all samples, sensitivity is defined as proportion of true positive among PSS mice, specificity is defined as proportion of true negative in non-PSS mice.

### Statistical Analysis

Data are represented as mean  $\pm$  SEM. Statistical significance between 2 groups was calculated using unpaired, 2-tailed Student's t-test.  $*P < .05$ ,  $**P < .01$ , and  $***P < .001$  were considered statistically significant. Analyses were performed using GraphPad Prism 9.

## Results

### Elevation in Serum, But Not Urinary, TBA Levels is Indicative of Murine PSS

C57BL/6 J mice are sporadically born with PSS.<sup>2–7</sup> To ensure scientific rigor, mice with PSS need to be identified and then stratified or excluded from study. Resin casting of hepatic portal circulation can be used to detect PSS (Figure 1A), but this method of detection could only be performed postmortem. Using serum TBA instead as a sole biomarker, we have determined that a cut-off value equal or above 40  $\mu\text{M}$ , a metric that also defines pathological cholemia in humans,<sup>15</sup> could reliably mark newborn mice with PSS prior to weaning from their mothers.<sup>2</sup> Serum TBA of mice with PSS remained elevated at 8 wk of age, irrespective of sex (Figure 1B). Moreover, serum TBA  $\geq 40 \mu\text{M}$  accurately identified endothelial-specific aryl hydrocarbon receptor (Ahr)-deficient mice ( $\text{Ahr}^{\text{fl/fl}}\text{Cre}^{\text{CdH5}}$ ), which develop PSS at 100% incidence,<sup>6</sup> relative to their non-PSS  $\text{Ahr}^{\text{fl/fl}}$  littermates (Figure 1B).

Next, we asked whether urinary TBA could be similarly employed as an independent, noninvasive biomarker of PSS, considering that urine is a major route for eliminating bile acids that are spilled over into circulation in patients with hepatobiliary diseases.<sup>16</sup> While urinary TBA was elevated in 8-wk-old WT and  $\text{Ahr}^{\text{fl/fl}}\text{Cre}^{\text{CdH5}}$  female PSS mice, such elevation was

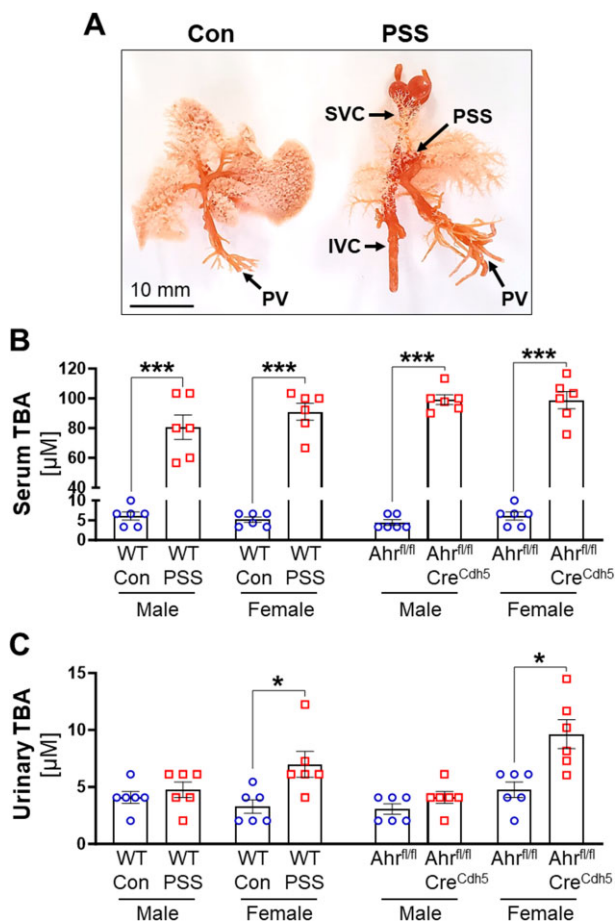


**Figure 1.** TBA levels in sera, but not urine, reliably mark mice with PSS. Male and female C57BL/6 J (alias wild-type, WT), Ahr<sup>fl/fl</sup> and Ahr<sup>fl/fl</sup>Cre<sup>Cdh5</sup> mice were assessed for serum TBA at 15 d of age. Based on serum TBA < or ≥ 40 µM, mice (n = 6) were respectively identified as non-PSS (Con) or PSS, respectively, for study. Note that all Ahr<sup>fl/fl</sup>Cre<sup>Cdh5</sup> mice have PSS. (A) Representative vascular casts of 8-wk-old WT Con and PSS mice (PV: portal vein, SVC: superior vena cava, IVC: inferior vena cava). At 8-wk-old, mice (n = 6) were measured for (B) serum TBA and (C) urinary TBA. Results were expressed as mean ± SEM. Student's t-test, \*P < .05, \*\*\*P < .001.

not observed in their male counterparts (Figure 1C). Such sexual disparity in urine TBA levels, though intriguing, is consistent with prior studies demonstrating that female rodents have a higher rate of bile acid sulfonation<sup>17–19</sup> and hydroxylation,<sup>20,21</sup> which increases the hydrophilicity and excretability of their bile acids via urine. Sexual disparity had also been noted in the expression of key enzymes involved bile acid biosynthesis, in part due to estrogen being an important regulator of bile acid biosynthesis, which increases the pool of hydrophilic bile acids in female mice.<sup>22</sup> These factors may have contributed to increase urinary TBA in female PSS mice and thus allowing its potential application for PSS detection for female mice.

### Murine PSS Associates With an Aberrant Urinary Excretion of Krebs Cycle Intermediates

Next, we asked whether mice with PSS exhibited elevation in urinary metabolites other than bile acids that could be explored as biomarkers for both male and female mice. To this end, we performed an untargeted <sup>1</sup>H-NMR-based metabolomic profiling

of urine collected from PSS and non-PSS C57BL/6 J mice. Prominent peaks denoting hippurate, a product of hepatic conjugation of glycine and benzoic acid derivatives, were significantly reduced in the urine collected from PSS mice (Figure 2A and B). This observation is consistent with our prior report on the reduced capacity of PSS mice to produce hippurate following oral benzoate challenge,<sup>2</sup> underscoring that their liver detoxification function was compromised.

More importantly, the urinary metabolome of PSS mice was marked by striking elevations of several Krebs cycle intermediates, that is, citrate, α-ketoglutarate, and fumarate (Figure 2A, C–E). Levels of urinary succinate, however, were comparable between PSS and non-PSS mice (Figure 2F). Such heightened excretion of exclusively mitochondria-derived metabolites could reflect a state of metabolic perturbation<sup>9</sup> and may be due to decreased utilization of Krebs cycle intermediates in energy metabolism, mitochondrial leakage or defect in the renal reabsorption of these metabolites. The physiologic underpinnings of such urine metabolome awaits further investigation. Nonetheless, these results indicate that PSS mice have a distinct urinary signature.

### PSS Increases Urinary Chelation of Iron

Organic carboxylic acids derived from the Krebs cycle are known to chelate metal ions, particularly iron.<sup>23</sup> Considering their abundance in the urine of PSS mice, we posited that colorimetric assessment of urinary siderophore activity (ie, iron chelation) via the Chrome Azurol Sulfonate (CAS) assay<sup>24</sup> could be used to identify PSS mice. When spotted on a CAS agar plate, urine from PSS mice formed an orange halo that was larger and distinctive than non-PSS urine (Figure 3A), semiquantitatively indicating that the former has more iron chelation activity. We applied known concentrations of sodium citrate to the CAS plate as positive controls; however, their orange halo differed in intensity relative to those formed by PSS urine (Figure 3A). Though this suggests that there were other iron chelators alongside citrate in the urine, this point did not detract from the consideration that CAS assay could be used to distinguish PSS from non-PSS mice.

Next, we repeated the assay using the quantitative CAS liquid method.<sup>24</sup> This led us to estimate that PSS urine had approximately ~1.6 to 2.2-fold more capacity to chelate iron compared to non-PSS urine (Figure 3B). To confirm that the assay measured iron chelation per se and was not confounded by other interfering substances, we tested for specificity by spiking the urine with ferric iron to neutralize its iron-chelating activity. As anticipated, the addition of ferric iron from 0.1 to 1.0 mM increasingly dampened the iron chelation exerted by PSS and non-PSS urine (Figure 3C and D). Iron chelation by PSS urine nevertheless remained higher than non-PSS urine even with addition of 0.1–0.5 mM ferric iron (Figure 3C and D). Taken together, these findings support the use of CAS assay as a potential means to screen for murine PSS.

### PSS Mice are Marked with Low Urinary pH

Another biochemical property of organic acids is their capacity to lower the pH of solutions. Though citrate (pK<sub>a1</sub> = 3.13, pK<sub>a2</sub> = 4.76, and pK<sub>a3</sub> = 6.40), α-ketoglutarate (pK<sub>a</sub> = 2.38), and fumarate (pK<sub>a1</sub> = 3.03, pK<sub>a2</sub> = 4.44) are weak acids, their high abundance in the urine of PSS mice may profoundly lower urinary pH. Indeed, by using semiquantitative pH test strips, we were able to rapidly identify mice with or without PSS. We found



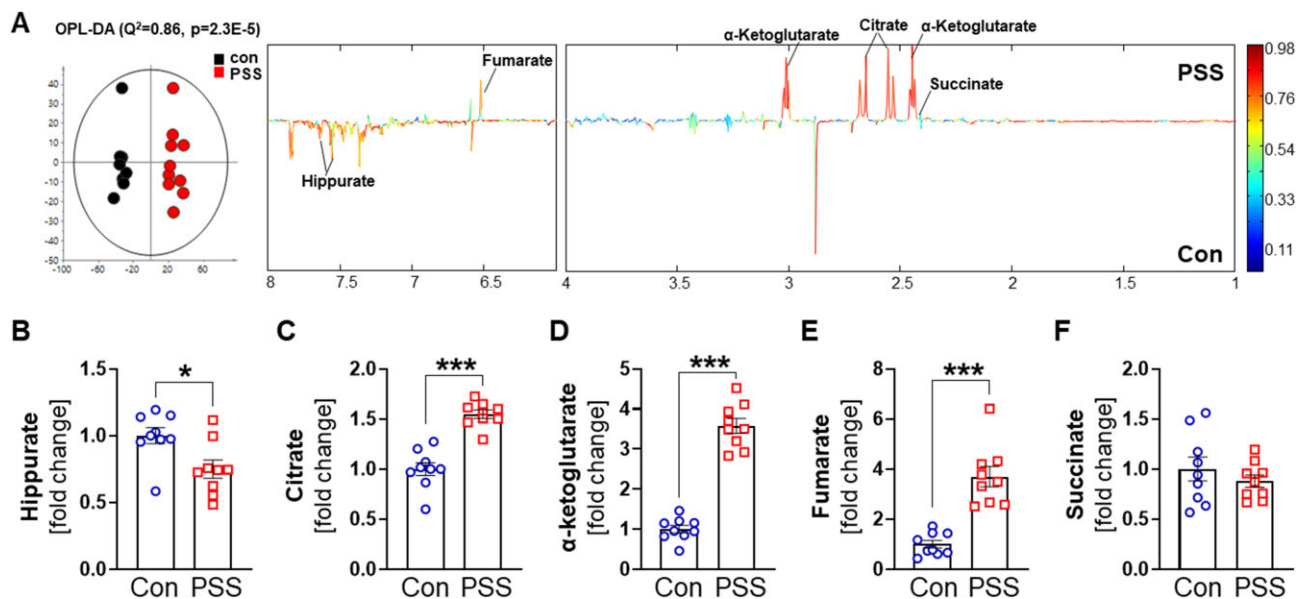


**Figure 2.** Urinary metabolome of mice with PSS displays a striking abundance of mitochondrial Krebs cycle intermediates. Urine from 24-wk-old male C57BL/6 J mice ( $n = 9$ ) was subjected to  $^1\text{H-NMR}$  analysis. (A) Urine NMR coefficient plot. Levels of urinary (B) hippurate, (C) citrate, (D)  $\alpha$ -ketoglutarate, (E) fumarate, and (F) succinate indicated as fold change analyzed via NMR. Results were expressed as mean  $\pm$  SEM. Student's t-test, \* $P < .05$ , \*\*\* $P < .001$ .

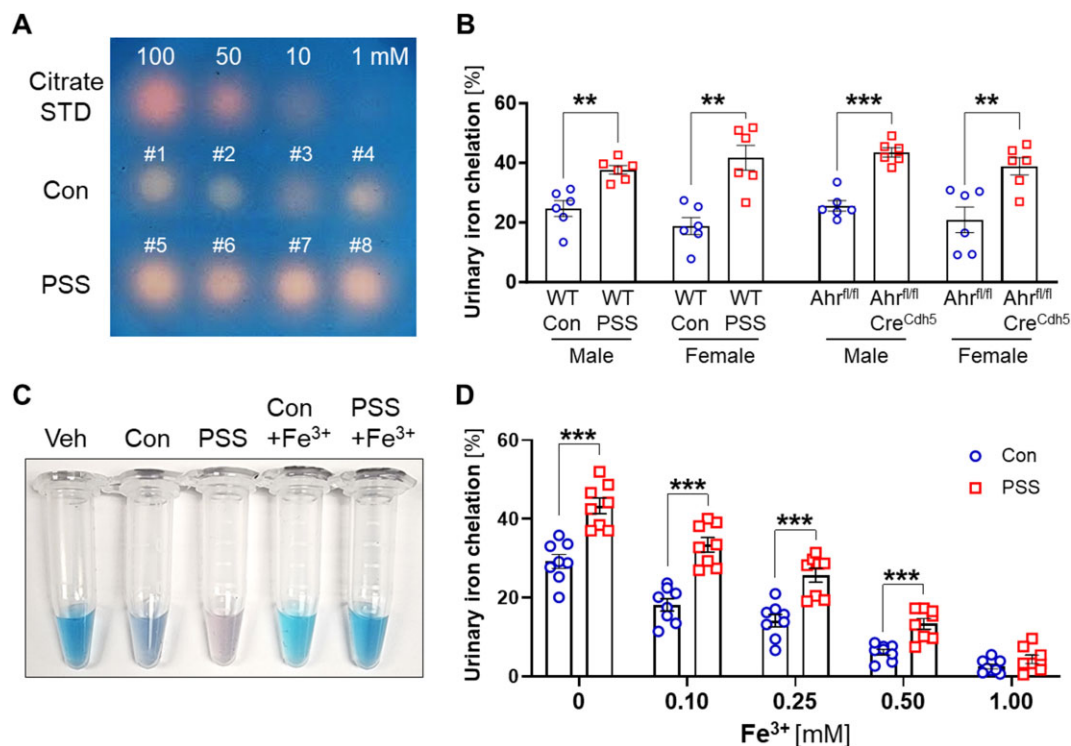


**Figure 3.** Higher urinary iron chelation activity as measured via CAS assay noninvasively identifies PSS mice. Urine from 8-wk-old male and female C57BL/6 J (WT),  $\text{Ahr}^{\text{fl/fl}}$  and  $\text{Ahr}^{\text{fl/fl}}\text{Cre}^{\text{Cdh5}}$  mice, which were preidentified as non-PSS (Con) or PSS mice ( $n = 6$ ), were subjected to CAS assay. (A) CAS agar plate spotted with  $3.0 \mu\text{L}$  urine showed orange halo formation, indicating iron chelation. Sodium citrate was used as a positive control on CAS agar plate. (B) Percent urinary iron chelation measured via the CAS liquid assay and the absorbance read at wavelength of 630 nm. (C) Image depicts the color of CAS reagent upon addition of Con and PSS urine that were spiked with or without  $0.5 \text{ mM FeCl}_3$ . (D) Percent urinary iron chelation of Con and PSS urine ( $n = 8$ ) that were preincubated with the indicated concentration of  $\text{FeCl}_3$  before assayed on CAS reagent. Results were expressed as mean  $\pm$  SEM. Student's t-test, \*\*\* $P < .01$ , \*\*\*\* $P < .001$ .

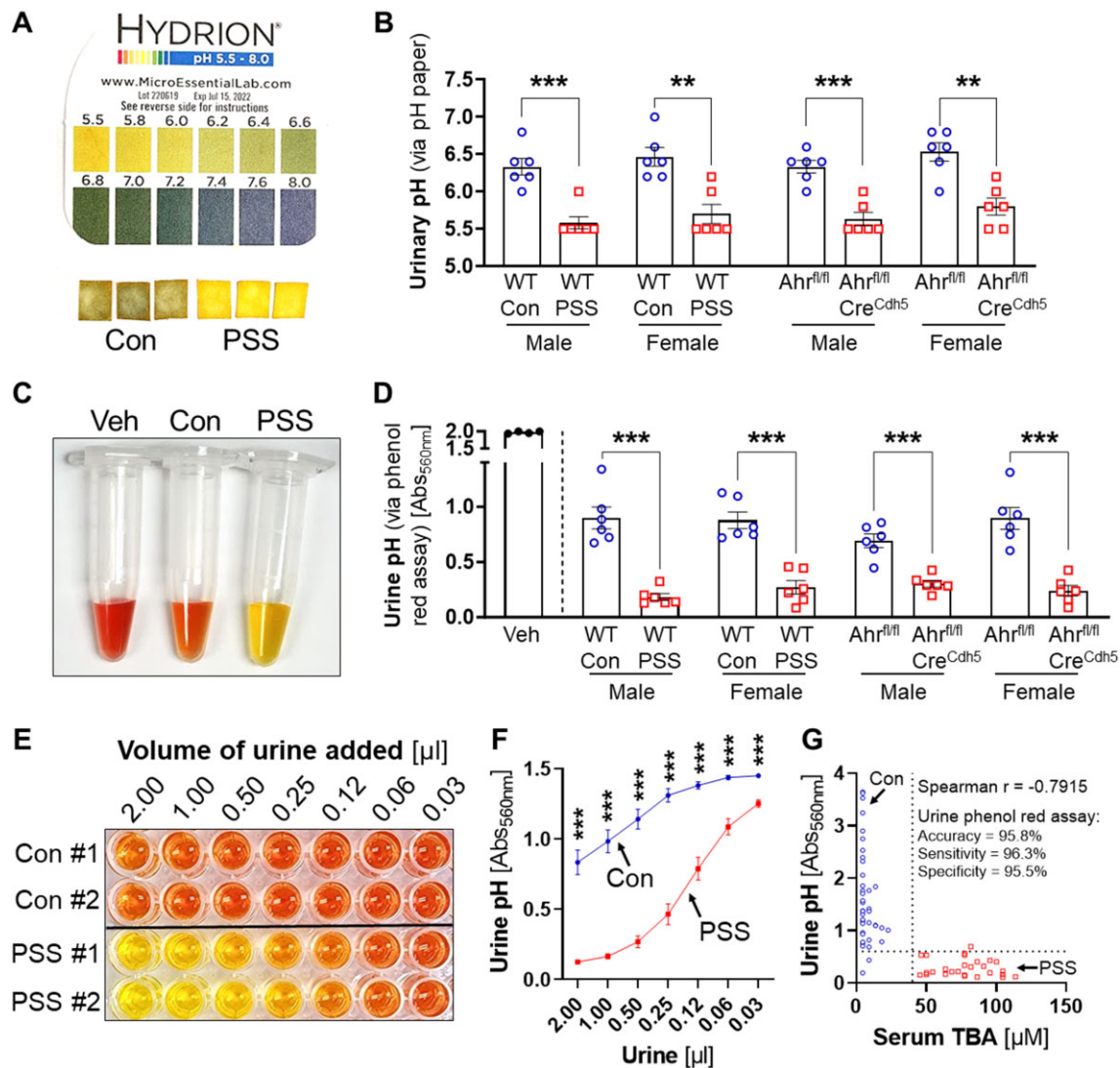


**Figure 4.** Low urinary pH is a specific, sensitive, and noninvasive biomarker for murine portosystemic shunt. Urinary pH of 8-wk-old male and female C57BL/6J (WT), *Ahr<sup>fl/fl</sup>* and *Ahr<sup>fl/fl</sup>Cre<sup>Cdh5</sup>* mice ( $n = 6$ ) was measured using pH test strips and phenol red assay. (A) Image and (B) bar graphs depict colorimetric readout of pH test strips in reference to a color chart. (C) Colorimetric readout observed upon addition of 2.0  $\mu$ l urine from non-PSS (Con) or PSS mice to 200  $\mu$ l phenol red (0.1 mg/mL) solution and the (D) pH change quantitated spectrophotometrically at wavelength of 560 nm. (E–F) Urine from 8-wk-old male C57BL/6J Con and PSS mice were serially diluted 2-fold to assess for detection limit. (E) Representative images depict the apparent color differences, and their (F) quantification ( $n = 6$ ) at wavelength of 560 nm. (G) Correlation plot of urine pH assessed via phenol red against serum TBA of Con ( $n = 44$ ; blue) and PSS ( $n = 27$ ; red) (Spearman  $r = -0.7915$ ;  $P$ -value  $< .001$ ). Using serum TBA  $\geq 40$   $\mu$ M and urine pH (absorbance at 560 nm)  $< 0.6$  as cut-offs, we noted the urine phenol red assay has an accuracy of 95.8% with false positive and false negative rates of 4.5% and 3.7%, respectively. Results were expressed as mean  $\pm$  SEM. Student's  $t$ -test, \*\* $P < .01$ , \*\*\* $P < .001$ .

that pH test strips with a narrow range were most reliable in discerning PSS urine with a pH of 5.5–6.0 (yellow color on pH strips) compared to non-PSS urine with a pH of 6.2–6.8 (green color on pH strips) (Figure 4A and B). Such differences, however, could not be visualized using pH test strips with a broad range or those with unit increments greater than 0.2 (data not shown). While the use of pH test strips with appropriate range is effective in identifying PSS mice rapidly, we noted that it can be at times challenging to discern the color difference in the narrow yellow–green range. Furthermore, despite the difference in the urine pH between non-PSS and PSS mice, their serum pH was comparable (data not shown).

We next asked whether other pH indicators could be harnessed in a more effective manner to screen urine from PSS

mice. Phenol red is ideal for this application not only because of its high sensitivity to pH changes, but also because its yellow–red range is more evident than those seen on pH test strips.<sup>25</sup> As anticipated, the addition of 2  $\mu$ l urine from PSS mice was sufficient to shift the color of 200  $\mu$ l phenol red solution (0.1 mg/mL, pH 7.4) to yellow (Figure 4C). Conversely, non-PSS mice urine modestly shifted the phenol red color to orange–red (Figure 4C). When the color change was measured on a spectrophotometer, we noted that the PSS samples have absorbance values that are  $\sim 3$ –5-fold lower when compared to non-PSS samples (Figure 4D). Taken together, these results demonstrate the feasibility of using urine pH, measured either via pH test strips or phenol red assay, to screen for mice with PSS.

## Urinary pH Test Via Phenol Red is Sensitive and Specific for Identification of PSS Mice

Among the assays we tested herein for screening PSS mice, the urine phenol red assay was superior in terms of simplicity, cost, and promptness in application. To further assess detection limit, we serially diluted the urine in phenol red solution. The lower limit of detection to discern PSS and non-PSS urine by visual colorimetric observation was approximated at 0.25  $\mu\text{L}$  urine (ie, 0.125% of assay volume) (Figure 4E). When using spectrophotometric measurements, the limit of detection can be extended to 0.03  $\mu\text{L}$  urine (ie, 0.015% assay volume) (Figure 4F). To test for assay accuracy, sensitivity, and specificity, we compared urine phenol red values against serum TBA of PSS mice, which were also subjected to postmortem confirmation of PSS via vascular casting. Consistent with prior results,<sup>2</sup> serum TBA  $\geq 40 \mu\text{M}$  was accurate for PSS diagnosis (Figure 4G). Urine phenol red assay was likewise effective with an accuracy of 95.8%, sensitivity of 96.3%, and specificity of 95.5% (Figure 4G). Taken together, these results demonstrate the feasibility of using urine as a liquid biopsy to screen for PSS in mice and of using phenol red assay as a reliable diagnostic test.

## Discussion

Since the first known clinical report of congenital PSS in humans more than 2 centuries ago,<sup>26</sup> efforts have been undertaken to diagnose PSS based on its anatomical location. Generally, PSS can be classified as extrahepatic (ie, Abernethy malformation) or intrahepatic (ie, *patent ductus venosus*). The intrahepatic PSS studied herein fits in the latter classification. Of note, during prenatal development of higher vertebrates, the *ductus venosus* serves as a fetal shunt that receives blood from the umbilical and portal vein and delivers blood into the hepatic vein. This allows maternal blood to bypass the fetal liver and, in doing so, provide immediate oxygenation to the fetal heart. After birth, the *ductus venosus* naturally closes between 2 and 18 d in humans<sup>27,28</sup> and within 48 h in mice.<sup>29</sup> Failure to close the *ductus venosus*, thus being “patent,” engenders a PSS that often persists throughout the lifespan of an individual or mouse.<sup>30</sup> The mechanisms that prevent closure of *ductus venosus* remain poorly understood; nevertheless, such anomaly has been associated with a dysregulation in AHR signaling. This premise is substantiated by numerous studies, which found that deficiency in genes related to the AHR pathway, namely *Ahr*,<sup>11,29</sup> *Ahr* nuclear translocator (*Arnt*),<sup>31</sup> *Ahr*-interacting protein (*Aip*),<sup>7</sup> heat shock protein 90 (*HSP90AA1*)<sup>32</sup> and nuclear factor erythroid 2-related factor 2 (*Nrf2*),<sup>5</sup> independently increases the incidence of PSS. Moreover, endothelial-specific deletion of *Ahr* was sufficient to increase PSS incidence to 100%,<sup>6</sup> suggesting that the inability to close *ductus venosus* is primarily driven by the endothelial cells lining the *ductus venosus*.

It has been estimated that congenital PSS occurs in humans with a prevalence of 1 out of 30 000 births. However, in fact, the frequently asymptomatic nature of PSS may cause most cases to be unrecognized and thus the true prevalence of human PSS may be much higher.<sup>33</sup> Despite being rare among humans, congenital PSS is a rather common vascular anomaly among certain breeds of dogs and cats.<sup>34</sup> Likewise, PSS occurs frequently among C57BL/6 J mice,<sup>1,2,4,5,8,9</sup> but it is not the only PSS-prone strain. We and others found that congenital PSS is also penetrant for strains such as C57BL/6NTac,<sup>2</sup> C57BL/6JOLA<sup>Hsd</sup>,<sup>10</sup> and 129/Ola.<sup>35</sup> Using serum TBA  $\geq 40 \mu\text{M}$  followed by resin casting of portal vasculature, we discovered that Swiss Webster mice,

which are outbred, are also susceptible to having PSS but at a rather low incidence (Figure 5A and B). Though the mechanistic basis of PSS remains largely unknown, it is rather enticing to consider that such mechanism(s) is likely well-conserved across multiple species given that they shared anatomical similarity in regards to *patent ductus venosus*.

From a broad biomedical research standpoint, the incidence of PSS undermines the notion that laboratory inbred mice exhibit minimal variance in physiology. PSS engenders what we consider a “leaky liver” that allows systemic spillover of not only bile acids, but also other noxious gut-derived microbial products such as lipopolysaccharide, flagellin, ammonia, and short-chain fatty acids. Consequences of such spillover are profound at the cellular and organ levels; as such, failure to account for this anomaly can impact data analysis, and interpretation. Cudalbu et al. cautioned that PSS mice have an abnormal neurochemical profile, which is characterized by elevation in cerebral glutamine presumably due to ammonia reaching the brain.<sup>1</sup> Further, PSS mice are exceptionally resistant to acetaminophen<sup>5</sup> and carbon tetrachloride<sup>8</sup> induced liver injury, but are singularly intolerant to any purified diets (*alias* compositionally defined diet) and dietary bile acids.<sup>10</sup> Therefore, these mice may pose a confounding variable that needs to be accounted for in research studying metabolism, toxicology and/or those that employ purified diets. As a case in point, we noted one study that strived to exclude PSS mice<sup>36</sup> and several other groups, despite not confirming for PSS, classified mice with PSS-like characteristics as anomalous.<sup>3,10,37,38</sup>

Despite being an anomaly, murine PSS is nonetheless an invaluable animal model with clinical relevance to humans with *patent ductus venosus*,<sup>33</sup> those who acquire spontaneous PSS due to liver cirrhosis,<sup>39</sup> and those who had underwent surgery for transjugular intrahepatic portosystemic shunt (TIPS; a surgically created shunt) to reduce portal hypertension.<sup>40</sup> In many aspects, PSS mice recapitulate phenotypes of their human counterparts,<sup>33</sup> including the propensity for hyperammonemia,<sup>1</sup> macro and micronutrient deficiencies,<sup>41</sup> and metabolic perturbations.<sup>2,9,10</sup> Hence, we posit that PSS mice could be further developed as the sought-after preclinical model to study novel treatments for a spectrum of PSS-related complications such as neonatal cholestasis and hepatic encephalopathy.<sup>33</sup> Of note, cholestatic liver injury has been observed in PSS mice given a NASH diet.<sup>8</sup> Moreover, we determined that PSS was the reason behind some mice developing liver cancer when fed a purified diet supplemented with refined inulin.<sup>3,42,43</sup> Notwithstanding the association between PSS and liver cancer risk being previously noted in humans,<sup>33</sup> our work provides empirical evidence on such a link and underscores intolerance to dietary fermentable fiber as an oncogenic trigger.<sup>2</sup> The potential of PSS mice being harnessed as a novel model for liver injury and cancer (via feeding inulin or NASH diet) would depend on whether or not we can accurately discern PSS mice.

Advances in ultrasound, computed tomography, and magnetic resonance imaging techniques have substantially improved clinical diagnosis of humans with PSS. Similar techniques have been applied for examining murine PSS<sup>1,9</sup>; however, their use as screening tools is restricted by requirements for specialized equipment and expertise that are not readily accessible to the wider scientific community. Accordingly, studies on murine PSS more often rely on using dye, resin, or microsphere injections to detect PSS.<sup>1,4,5,11</sup> Such approaches can only be performed postmortem and therefore have limited utility for screening/tracking live mice. Previously, we have



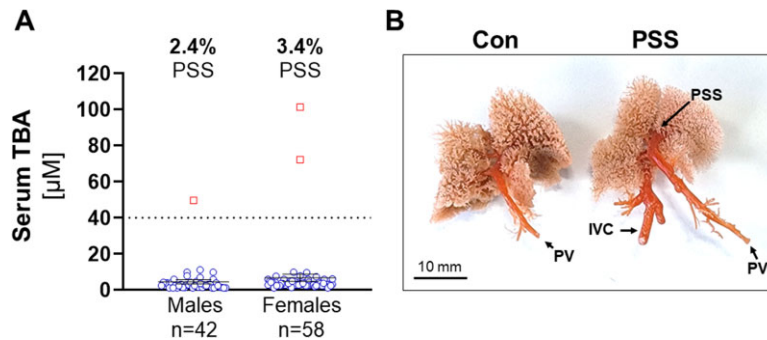


**Figure 5.** Swiss Webster mice are prone to have PSS at a rather low incidence. Swiss Webster male ( $n = 42$ ) and female ( $n = 58$ ) mice were screened for (A) serum TBA at 15 d of age, whereafter mice with serum TBA  $\geq 40 \mu\text{M}$  were confirmed for PSS using resin casting of portal vasculature. (B) Representative vascular casts of 8-wk-old Swiss Webster non-PSS (Con) and PSS mice (PV: portal vein, SVC: superior vena cava, IVC: inferior vena cava).

demonstrated that serum TBA  $\geq 40 \mu\text{M}$  is a *bona fide* biomarker that can be used, in a nonterminal manner, to discern PSS mice by day 15 of age.<sup>2</sup> Our group, as well as others, have also found that PSS mice exhibit hallmark characteristics such as hypoglycemia, hypolipidemia (eg, hypocholesterolemia and hypotriglyceridemia), small liver, and the proneness to develop rapid onset of cholestatic liver injury [eg, elevated serum alanine transaminase (ALT)] and hyperbilirubinemia in response to compositionally defined diets.<sup>2,8-10</sup> Elevation in circulating ammonia may be a potential PSS biomarker; however, it has been noted to be rather ineffective in differentiating PSS from non-PSS mice.<sup>1</sup> The aforementioned parameters could certainly be monitored in a combinatorial manner to identify PSS mice, but testing for them may be a technical challenge for laboratories that are not trained to collect sera without hemolysis and measure the relevant serologic parameters (eg, TBA, glucose, ALT, and bilirubin). A more tractable screening approach is therefore warranted and we undertook this study to determine whether urine, as a highly accessible biofluid, could be used for PSS screening.

Urinary metabolome of PSS mice revealed that organic acids, namely citrate,  $\alpha$ -ketoglutarate, and fumarate, were strikingly enriched at a magnitude greater than other urinary metabolites. With the knowledge that these metabolites can chelate iron and lower pH, we evaluated 3 PSS screening approaches, that is, urinary CAS, pH test strips, and phenol red assays. These colorimetric assays use inexpensive and commercially available reagents, and the readout can be obtained by direct observation without needing any additional instrumentation. Among the tests examined in this study, CAS assay is less favored because urinary iron chelation occurs gradually and thus needs to be incubated for some time before results can be perceived. Conversely, pH tests offer immediate results and, moreover, the colorimetric readout remains stable over time. As such, we envision pH tests to be more suited for large-scale rapid screenings that can either be performed in bulk (eg, 96-well format) or 1 sample at a time. Notwithstanding these tests being highly accurate and sensitive for murine PSS, whether they have a similar utility for screening human PSS remains to be tested and thus warrants future investigation.

Taken together, our study herein demonstrates the feasibility of using urine iron chelation and urine pH as novel biomarkers of murine PSS. We envision such approaches would enable the scientific community to reliably identify PSS mice in a cost- and time-effective manner and exclude them from studies to maintain scientific rigor. Perhaps more importantly,

timely identification of PSS mice would allow them to be leveraged in research that can advance our limited understanding on the pathophysiology of PSS and its associated consequences.

## Acknowledgments

Graphical abstract was created with BioRender.com.

## Authors Contribution

B.S.Y., B.J., and M.V-K. designed research; B.S.Y., R.M.G., P.S., M.R.K., and Y.T. performed research; B.S.Y., Y.T., I.O., A.D.P., A.T.G., B.J., and M.V-K. analyzed data; and B.S.Y., A.T.G., B.J., and M.V-K. wrote the paper.

## Funding

This work was supported by the National Institute of Health (NIH), National Cancer Institute (R01 CA219144) to M.V-K., and the USDA National Institute of Food and Agriculture and Hatch Appropriations under Project #PEN04772 and Accession #7000371 and grant U01DK119702 to A.D.P. B.S.Y. is supported by the Postdoctoral Fellowship (Award# 831112) from American Heart Association (AHA). R.M.G. is supported by the National Cancer Institute, NIH (Award# F31 CA260842). P.S. is supported by the Career Development Awards (Award# 854385 and 855256, respectively) from Crohn's and Colitis Foundation (CCF) and AHA. I.O. is supported by a grant from the National Heart, Lung, and Blood Institute (R00 HL153896).

## Conflict of Interest

None declared.

## Data Availability

The data that support the findings of this study are available from the corresponding authors upon reasonable request.

## References

1. Cudalbu C, McLin VA, Lei H, et al. The C57BL/6 J mouse exhibits sporadic congenital portosystemic shunts. *PLoS One*. 2013;8(7):e69782.



2. Yeoh BS, Saha P, Golonka RM, et al. Enterohepatic shunt-driven cholemia predisposes to liver cancer. *Gastroenterology*. 2022;163(6):1658–1671.e16.
3. Singh V, Yeoh BS, Chassaing B, et al. Dysregulated microbial fermentation of soluble fiber induces cholestatic liver cancer. *Cell*. 2018;175(3):679–694.e622.
4. Maroni L, Hohenester SD, van de Graaf SFJ, et al. Knockout of the primary sclerosing cholangitis-risk gene *Fut2* causes liver disease in mice. *Hepatology*. 2017;66(2):542–554.
5. Skoko JJ, Wakabayashi N, Noda K, et al. Loss of *Nrf2* in mice evokes a congenital intrahepatic shunt that alters hepatic oxygen and protein expression gradients and toxicity. *Toxicol Sci*. 2014;141(1):112–119.
6. Walisser JA, Glover E, Pande K, Liss AL, Bradfield CA. Aryl hydrocarbon receptor-dependent liver development and hepatotoxicity are mediated by different cell types. *Proc Natl Acad Sci USA*. 2005;102(49):17858–17863.
7. Lin BC, Nguyen LP, Walisser JA, Bradfield CA. A hypomorphic allele of aryl hydrocarbon receptor-associated protein-9 produces a phenocopy of the AHR-null mouse. *Mol Pharmacol*. 2008;74(5):1367–1371.
8. Meng L, Goto M, Tanaka H, et al. Decreased portal circulation augments fibrosis and ductular reaction in nonalcoholic fatty liver disease in mice. *Am J Pathol*. 2021;191(9):1580–1591.
9. Soares AF, Lei H. Non-invasive diagnosis and metabolic consequences of congenital portosystemic shunts in C57BL/6 J mice. *NMR Biomed*. 2018;31(2):e3873.
10. Ronda O, van de Heijning BJM, de Bruin A, et al. Spontaneous liver disease in wild-type C57BL/6J *OlaHsd* mice fed semisynthetic diet. *PLoS One*. 2020;15(9):e0232069.
11. Lahvis GP, Lindell SL, Thomas RS, et al. Portosystemic shunting and persistent fetal vascular structures in aryl hydrocarbon receptor-deficient mice. *Proc Natl Acad Sci USA*. 2000;97(19):10442–10447.
12. Huang C, Lei H, Zhao X, Tang H, Wang Y. Metabolic influence of acute cyadox exposure on Kunming mice. *J Proteome Res*. 2013;12(1):537–545.
13. Schwyn B, Neilands JB. Universal chemical assay for the detection and determination of siderophores. *Anal Biochem*. 1987;160(1):47–56.
14. Trevethan R. Sensitivity, specificity, and predictive values: foundations, pliabilities, and pitfalls in research and practice. *Front Public Health*. 2017;5:307. <https://www.frontiersin.org/articles/10.3389/fpubh.2017.00307/full>.
15. Glantz A, Marschall HU, Mattsson LA. Intrahepatic cholestasis of pregnancy: relationships between bile acid levels and fetal complication rates. *Hepatology*. 2004;40(2):467–474.
16. Stiehl A, Raedsch R, Rudolph G, Gundert-Remy U, Senn M. Biliary and urinary excretion of sulfated, glucuronidated and tetrahydroxylated bile acids in cirrhotic patients. *Hepatology*. 1985;5(3):492–495.
17. Barnes S, Burhol PG, Zander R, Haggstrom G, Settine RL, Hirschowitz BI. Enzymatic sulfation of glycochenodeoxycholic acid by tissue fractions from adult hamsters. *J Lipid Res*. 1979;20(8):952–959.
18. Hammerman KJ, Chen LJ, Fernandez-Corugedo A, Earnest DL. Sex differences in hepatic sulfation of tauroolithocholate in the rat. *Gastroenterology*. 1978;75(6):1021–1025.
19. Kane RE, Chen LJ, Herbst JJ, Thaler MM. Sexual differentiation of rat hepatic bile salt sulfotransferase isoenzymes. *Pediatr Res*. 1988;24(2):247–253.
20. Kuroki S, Muramoto S, Kuramoto T, Hoshita T. Sex differences in gallbladder bile acid composition and hepatic steroid 12 alpha-hydroxylase activity in hamsters. *J Lipid Res*. 1983;24(12):1543–1549.
21. Carlson SE, Mitchell AD, Goldfarb S. Sex-related differences in diurnal activities and development of hepatic microsomal 3-hydroxy-3-methylglutaryl coenzyme A reductase and cholesterol 7alpha-hydroxylase. *Biochim Biophys Acta*. 1978;531(1):115–124.
22. Phelps T, Snyder E, Rodriguez E, Child H, Harvey P. The influence of biological sex and sex hormones on bile acid synthesis and cholesterol homeostasis. *Biol Sex Differ*. 2019;10(1):52.
23. Harrar NJ, Germann FEE. A study of organic-acid iron solutions. III. *J Phys Chem*. 1932;36(2):688–695.
24. Xiao X, Yeoh BS, Saha P, et al. Modulation of urinary siderophores by the diet, gut microbiota and inflammation in mice. *J Nutr Biochem*. 2017;41:25–33. <https://pubmed.ncbi.nlm.nih.gov/27951517/>.
25. Raffay R, Husin N, Omar AF. Spectrophotometry and colorimetry profiling of pure phenol red and cell culture medium on pH variation. *Color Technol*. 2022;138(6):640–659.
26. Abernethy J. Account of two instances of uncommon formation in the viscera of the human body: from the Philosophical Transactions of the Royal Society of London. *Med Facts Obs*. 1797;7:100–108. <https://pubmed.ncbi.nlm.nih.gov/29106224/>.
27. Fugelseth D, Lindemann R, Liestol K, Kiserud T, Langslet A. Postnatal closure of ductus venosus in preterm infants < or = 32 weeks. An ultrasonographic study. *Early Hum Dev*. 1998;53(2):163–169.
28. Loberant N, Barak M, Gaitini D, Herskovits M, Ben-Elisha M, Roguin N. Closure of the ductus venosus in neonates: findings on real-time gray-scale, color-flow doppler, and duplex doppler sonography. *AJR Am J Roentgenol*. 1992;159(5):1083–1085.
29. Lahvis GP, Pyzalski RW, Glover E, Pitot HC, McElwee MK, Bradfield CA. The aryl hydrocarbon receptor is required for developmental closure of the ductus venosus in the neonatal mouse. *Mol Pharmacol*. 2005;67(3):714–720.
30. Paganelli M, Lipsich JE, Sciveres M, Alvarez F. Predisposing factors for spontaneous closure of congenital portosystemic shunts. *J Pediatr*. 2015;167(4):931–935.e912.
31. Walisser JA, Bunger MK, Glover E, Harstad EB, Bradfield CA. Patent ductus venosus and dioxin resistance in mice harboring a hypomorphic *Arnt* allele. *J Biol Chem*. 2004;279(16):16326–16331.
32. van Steenbeek FG, Spee B, Penning LC, et al. Altered subcellular localization of heat shock protein 90 is associated with impaired expression of the aryl hydrocarbon receptor pathway in dogs. *PLoS One*. 2013;8(3):e57973.
33. Bernard O, Franchi-Abella S, Branchereau S, Pariente D, Gauthier F, Jacquemin E. Congenital portosystemic shunts in children: recognition, evaluation, and management. *Semin Liver Dis*. 2012;32(04):273–287.
34. Konstantinidis AO, Adamama-Moraitou KK, Patsikas MN, Papazoglou LG. Congenital portosystemic shunts in dogs and cats: treatment, complications and prognosis. *Vet Sci*. 2023;10(5):346.
35. Coulson PS, Wilson RA. Portal shunting and resistance to *Schistosoma mansoni* in 129 strain mice. *Parasitology*. 1989;99(3):383–389.

36. Takiyama T, Sera T, Nakamura M, et al. A maternal high-fat diet induces fetal origins of NASH-HCC in mice. *Sci Rep*. 2022;**12**(1):13136.
37. Tarasco E, Pellegrini G, Whiting L, Lutz TA. Phenotypical heterogeneity in responder and nonresponder male ApoE\*3Leiden.CETP mice. *Am J Physiol Gastrointest Liver Physiol*. 2018;**315**(4):G602–G617.
38. Burcelin R, Crivelli V, Dacosta A, Roy-Tirelli A, Thorens B. Heterogeneous metabolic adaptation of C57BL/6 J mice to high-fat diet. *Am J Physiol Endocrinol Metab*. 2002;**282**(4):E834–E842.
39. Vidal-Gonzalez J, Quiroga S, Simon-Talero M, Genesca J. Spontaneous portosystemic shunts in liver cirrhosis: new approaches to an old problem. *Therap Adv Gastroenterol*. 2020;**13**:1756284820961287. <https://pubmed.ncbi.nlm.nih.gov/33062057/>.
40. Tripathi D, Stanley AJ, Hayes PC, et al. Transjugular intrahepatic portosystemic stent-shunt in the management of portal hypertension. *Gut*. 2020;**69**(7):1173–1192.
41. Golonka RM, San Yeoh B, Li Y, et al. Fermentable fibers induce rapid macro- and micronutrient depletion in toll-like receptor 5-deficient mice. *Am J Physiol Gastrointest Liver Physiol*. 2020;**318**(5):G955–G965.
42. Chandrashekar DS, Golonka RM, Yeoh BS, et al. Fermentable fiber-induced hepatocellular carcinoma in mice recapitulates gene signatures found in human liver cancer. *PLoS One*. 2020;**15**(6):e0234726.
43. Singh V, Yeoh BS, Abokor AA, et al. Vancomycin prevents fermentable fiber-induced liver cancer in mice with dysbiotic gut microbiota. *Gut Microbes*. 2020;**11**(4):1077–1091.